Atmos. Chem. Phys. Discuss., 9, 8635–8665, 2009
www.atmos-chem-phys-discuss.net/9/8635/2009/

Atmospheric Chemistry and Physics Discussions

This discussion paper is/has been under review for the journal *Atmospheric Chemistry and Physics (ACP)*. Please refer to the corresponding final paper in *ACP* if available.

Aerosol- and updraft-limited regimes of cloud droplet formation: influence of particle number, size and hygroscopicity on the activation of cloud condensation nuclei (CCN)

P. Reutter[1,2], J. Trentmann[2,*], H. Su[1], M. Simmel[3], D. Rose[1], H. Wernli[2], M. O. Andreae[1], and U. Pöschl[1]

[1]Max Planck Institute for Chemistry, Biogeochemistry Department, Mainz, Germany
[2]Institute for Atmospheric Physics, Johannes Gutenberg University Mainz, Mainz, Germany
[3]Leibniz Institute for Tropospheric Research, Leipzig, Germany
[*]German Weather Service, DWD Offenbach, Germany

Received: 3 March 2009 – Accepted: 20 March 2009 – Published: 1 April 2009

Correspondence to: P. Reutter (preutter@uni-mainz.de)

Published by Copernicus Publications on behalf of the European Geosciences Union.

Abstract

We have investigated the formation of cloud droplets under (pyro-)convective conditions using a cloud parcel model with detailed spectral microphysics and with the κ-Köhler model approach for efficient and realistic description of the cloud condensation nucleus (CCN) activity of aerosol particles. Assuming a typical biomass burning aerosol size distribution (accumulation mode centred at 120 nm), we have calculated initial cloud droplet number concentrations (N_{CD}) for a wide range of updraft velocities (w=0.5–20 m s^{-1}) and aerosol particle number concentrations (N_{CN}=10^3–10^5 cm^{-3}) at the cloud base. Depending on the ratio between updraft velocity and particle number concentration (w/N_{CN}), we found three distinctly different regimes of CCN activation and cloud droplet formation:

1. An aerosol-limited regime that is characterized by high w/N_{CN} ratios ($>\approx 10^{-3}$ m s^{-1} cm^3), high maximum values of water vapour supersaturation ($S_{max}>\approx$0.5%), and high activated fractions of aerosol particles ($N_{CD}/N_{CN}>\approx$90%). In this regime N_{CD} is directly proportional to N_{CN} and practically independent of w.

2. An updraft-limited regime that is characterized by low w/N_{CN} ratios ($<\approx 10^{-4}$ m s^{-1} cm^3), low maximum values of water vapour supersaturation ($S_{max}<\approx$0.2%), and low activated fractions of aerosol particles ($N_{CD}/N_{CN}<\approx$20%). In this regime N_{CD} is directly proportional to w and practically independent of N_{CN}.

3. An aerosol- and updraft-sensitive regime, which is characterized by parameter values in between the two other regimes and covers most of the conditions relevant for pyro-convection. In this regime N_{CD} depends non-linearly on both N_{CN} and w.

In sensitivity studies we have tested the influence of aerosol particle hygroscopicity on N_{CD}. Within the range of effective hygroscopicity parameters that is characteristic for continental atmospheric aerosols ($\kappa\approx$0.05–0.6), we found that N_{CD} depends

ACPD
9, 8635–8665, 2009

rather weakly on the actual value of κ. Only for aerosols with very low hygroscopicity (κ<0.05) and in the updraft-limited regime also for aerosols with higher than average hygroscopicity (κ>0.3) did the relative differential quotients $(\Delta N_{CD}/N_{CD})/(\Delta\kappa/\kappa)$ exceed values of ~0.2, indicating that a 50% difference in κ would change N_{CD} by more than 10%. Realistic changes in the aerosol particle size distribution had practically no effect on the aerosol-limited regime and limited influence on the aerosol- and updraft sensitive regime ($\Delta N_{CD}/N_{CD}$<30%) but can have strong effects at low supersaturation in the updraft-limited regime ($\Delta N_{CD}/N_{CD}$>30% at $S_{\max}$<0.1%). Overall, the results of this and related studies suggest that the variability of initial cloud droplet number concentration in (pyro-)convective clouds is mostly dominated by the variability of updraft velocity and aerosol particle number concentration in the accumulation mode. Coarse mode particles and the variability of particle composition and hygroscopicity appear to be play major roles only at low supersaturation in the updraft-limited regime of CCN activation ($S_{\max}$<0.2%).

1 Introduction

Clouds cover about 60% of the Earth's surface and have a strong influence on the global radiative balance, water cycle and climate (IAPSAG, 2007; IPCC, 2007). Deep convective clouds play an important role in the vertical redistribution of energy and moisture, especially in the tropics (Wang, 2003; Jiang et al., 2004). At mid-latitudes, deep convection is often associated with heavy rain events and severe weather. Hence, modifications of convective cloud properties can affect weather and climate on local and global scales (Rosenfeld, 2006).

A crucial factor for the dynamical and microphysical evolution of clouds is the activation of aerosol particles as cloud condensation nuclei (CCN), i.e., their hygroscopic growth into aqueous droplets that can freely grow by condensation of water vapor. Enhancing the number of aerosol particles that can serve as CCN generally leads to more and smaller cloud droplets at cloud base. It is well established that for shallow clouds,

ACPD
9, 8635–8665, 2009

the precipitation efficiency is reduced when the aerosol concentration increases (e.g. Rosenfeld et al., 2000; Penner et al., 2004; Andreae and Rosenfeld, 2008). For deep convective clouds, the consequences of enhanced aerosol concentration are nonlinear and depend strongly on meteorological parameters (e.g. Khain et al., 2008; Rosenfeld et al., 2008).

Transport through deep convective clouds has been identified as a relevant source for upper tropospheric/lower stratospheric (UT/LS) aerosol (e.g. Andreae et al., 2001; Wang, 2003; Luderer et al., 2006). The number of aerosol particles released into the UT/LS region depends on the number of activated aerosol particles and on the microphysical evolution of deep convective clouds (nucleation and precipitation scavenging), which, in turn, is also modified by aerosol activation at cloud base.

Pyro-convection, i.e., deep convective clouds that form above wildfires, is one of the most extreme forms of atmospheric deep convection. Observational and modeling studies have shown the extraordinary dynamical and microphysical properties of deep pyro-clouds (e.g. Fromm and Servranckx, 2003; Fromm et al., 2005; Trentmann et al., 2006; Rosenfeld et al., 2007) and their ability to transport substantial amounts of aerosol into the UT/LS (Fromm et al., 2005; Luderer et al., 2007). However, the relevant processes in pyro-clouds, including CCN activation at the cloud base, are not yet fully characterized and understood.

The main parameters governing CCN activation and initial cloud droplet growth are the number, size and hygroscopicity of aerosol particles as well as the updraft velocity at the cloud base and the resulting water vapour supersaturation. In most earlier studies of cloud droplet formation, the number concentration of aerosol particles did not exceed 10^4 cm^{-3} (e.g. Hjelmfelt et al. 1978; Hegg, 1999; Nenes et al., 2001; Feingold, 2003; Lance et al., 2004; Lohmann et al., 2004; Ervens et al., 2005; Segal and Khain, 2006; Kivekas et al., 2008; Cubison et al., 2008; Altaratz et al., 2008). This is realistic for regions with low or moderate air pollution, but in biomass burning plumes the aerosol particle number concentrations can reach up to ~10^5 cm^{-3} (Andreae et al., 2004; Reid et al., 2005; Janhäll et al., 2009).

ACPD
9, 8635–8665, 2009

To investigate and characterize the process of CCN activation in (pyro-)convective clouds, we have performed cloud parcel model simulations for a wide range of conditions, including the high updraft velocities and aerosol particle number concentrations observed over wildfires (0.5–20 m s^{-1}, 10^3–10^5 cm^{-3}). Moreover, we have implemented and tested the κ-Köhler model approach as an efficient and realistic new way of describing the CCN activity of aerosol particles with complex chemical composition as emitted from biomass burning (Petters and Kreidenweis, 2007; Pöschl et al., 2009), rather than using unrealistic surrogates species like sodium chloride (e.g., Segal and Khain, 2006).

In Sect. 2 of this paper we describe the applied cloud parcel and Köhler models (hygroscopicity parameter and osmotic coefficient formalisms), and we present the results of test calculations performed for comparison and validation against an alternative cloud parcel model with spectral microphysics (Segal and Khain, 2006). In Sect. 3 we present and discuss the results of model calculations exploring the dependence of cloud droplet number concentration on updraft velocity and aerosol particle number concentration as well as particle size and hygroscopicity.

2 Methods

2.1 Cloud parcel model

The cloud parcel model used in this study has been developed by Simmel et al. (2002) and contains a detailed spectral description of cloud microphysics (Simmel and Wurzler, 2006; Diehl et al., 2006, 2007). Based on a given dry aerosol size distribution, the model initially calculates the equilibrium aerosol size distribution at the relative humidity prescribed for the start of the simulation. As the air parcel rises with a prescribed vertical velocity, the model simulates the expansion and cooling of air as well as the resulting changes in relative humidity and the related hygroscopic growth of aerosol particles and further condensational growth of cloud droplets. Collision-coalescence

ACPD
9, 8635–8665, 2009

and entrainment processes were not included in our simulations, which are focused on CCN activation and initial growth of cloud droplets at the cloud base. Model test runs including collision-coalescence showed that coagulation can indeed be neglected at the early stages of cloud evolution investigated in this study (relative deviations ≤1%).

Particle growth rates were calculated according to the following equation (Pruppacher and Klett, 1997; Simmel and Wurzler, 2006):

$$\frac{dm}{dt} = \frac{4\pi r \left(s_\infty - s_{eq}\right)}{\left(\frac{L_V}{R_V T} - 1\right)\frac{L_V}{K^* T} + \frac{R_V T}{e_{s,w}(T) D^*}} \quad (1)$$

where m is the particle mass, t the simulation time, L_V the latent heat of condensation ($2.50078 \times 10^6\,\mathrm{J\,kg^{-1}}$), R_V the gas constant for water vapor ($461.5\,\mathrm{J\,kg^{-1}\,K^{-1}}$), K^* the modified thermal conductivity of air ($\mathrm{W\,m^{-1}\,K^{-1}}$), $e_{s,w}$ the saturation water vapor pressure, D^* the modified diffusion coefficient for water vapor in air ($\mathrm{m^2\,s^{-1}}$), s_∞ the saturation ratio of the surrounding air and s_{eq} the equilibrium water vapor saturation ratio at the particle/air interface. For more details and parameterizations of K^* and D^* see Simmel and Wurzler (2006).

Both aerosol particle and cloud droplet size and growth are described on a common spectral grid. The simulations presented here were carried out using 264 logarithmically equidistant bins between 1 nm and 3.5 mm and a time step of dt=0.01 s. The weighting coefficient for the redistribution of mass between the size bins after each time step was set to a=0.6 (Simmel and Wurzler, 2006). The prognostic parameters include liquid water mass and particle number for each size bin.

The input parameters required to initialize the simulations are: (1) the initial meteorological conditions (temperature, pressure, relative humidity); (2) the updraft velocity of the air parcel; (3) the dry aerosol particle number size distribution; and (4) a set of parameters characterizing the hygroscopicity of the particle material according to Köhler theory (effective hygroscopicity parameter, κ, or a combination of stoichiometric dissociation coefficient and osmotic coefficient, $\nu_s \Phi_s$; see Sect. 2.2).

ACPD
9, 8635–8665, 2009

All model simulations were initialized with a temperature of 285.20 K, a pressure of 950 hPa, and a relative humidity of 95% (Simmel and Wurzler, 2006). They were carried through with a constant vertical velocity (w), and stopped upon reaching a liquid water content (LWC) of 0.8 g kg^{-1}. In different runs the vertical velocity (w), initial aerosol particle number concentration (N_{CN}), size distribution, and hygroscopicity parameter were varied as detailed below.

The highest value of the water vapor supersaturations calculated in the course of each simulation (S=(s_∞-1) 100%) was reported as the maximum supersaturation $S_{\max}$ (for an exemplary profile of S see Fig. 1). The cloud droplet number concentrations (N_{CD}) and activated particle fractions (N_{CD}/N_{CN}) reported below were determined from the model output at the end of the simulation. Particles were counted as cloud droplets when the diameter is equal or larger than the critical droplet diameter corresponding to the maximum supersaturation of each parcel model run (Seinfeld and Pandis; 2006; $D_{\mathrm{wet},c}=\frac{2A}{3\ln S_c}$ with $A=\frac{4\sigma M_w}{RT\rho_w}$, and $S_c=S_{\max}$; for symbols and parameter values see Sect. 2.2 and Rose et al., 2008a). Under the model conditions investigated in this study (constant updraft, no entrainment, no coagulation), the results are the same when using the maximum value or the final value of supersaturation for the calculation of $D_{\mathrm{wet},c}$. Different approaches of cloud droplet counting are required and will be discussed in follow-up studies including coagulation, entrainment and variable updraft velocities.

2.2 Köhler models

According to Köhler theory, the equilibrium water vapor saturation ratio s_{eq} is given by

$$s_{eq} = a_w \times Ke \tag{2}$$

where a_w denotes the water activity or Raoult term, and Ke is the Kelvin term. In this study we have tested two different approaches of describing the influence of aerosol chemical composition and hygroscopicity on a_w: an effective hygroscopicity parameter (κ) Köhler model and an osmotic coefficient (OS) reference model which is more

ACPD
9, 8635–8665, 2009

accurate but also more complex as detailed by Rose et al. (2008a). In the OS Köhler model, a_w is given by

$$a_w = \exp\left(-\nu_s \Phi_s \mu_s M_w\right) \tag{3}$$

where ν_s, Φ_s and μ_s are the stoichiometric dissociation number, osmotic coefficient and molality of the aerosol particle material (solute), respectively, and M_w is the molar mass of water. In the test simulations for sodium chloride particles (Sect. 2.4), we have used ν_s=2 and the parameterization of Pitzer and Mayorga (1973) for Φ_s (OS1 model of Rose et al., 2008a) In the κ-Köhler model a_w is given by

$$a_w = \frac{1}{1 + \kappa \frac{V_s}{V_w}} \tag{4}$$

where κ and V_s are the effective hygroscopicity parameter and the volume of dry particulate matter ($V_S = \frac{4}{3}\pi \times r_s^3$, with r_s the radius of the particles), and V_w is the volume of water in the aqueous particle/droplet ($V_W = \frac{4}{3}\pi \times r_w^3$, with r_w the radius of the wet fraction). Characteristic values of κ are 0 for completely insoluble particles, 0.6 for $(NH_4)_2SO_4$ and 1.28 for NaCl (Petters and Kreidenweis, 2007; Rose et al., 2008a). The hygroscopicity parameters of biomass burning aerosols range from 0.01 for freshly emitted smoke containing mostly soot particles to 0.55 for aerosol from grass burning, and the average value of κ in polluted continental air is 0.3±0.1 (Andreae and Rosenfeld, 2008; Rose et al., 2008b; Pöschl et al., 2009).

In test simulations for sodium chloride particles (Sect. 2.3), we have used κ=1.28 and ρ_s=2165 kg m^{-3} (EH1 model of Rose et al., 2008a). For the simulation of real atmospheric aerosols (rural and biomass burning) we have used κ=0.2 and ρ_s=1300 kg m^{-3}. The Kelvin term was described by

$$Ke = \exp\left(\frac{2\sigma}{R_V T \rho_w r_{\text{wet}}}\right) \tag{5}$$

ACPD
9, 8635–8665, 2009

where σ and r_{wet} are the surface tension and radius of the aqueous particle/droplet respectively. R_V=461.5 J kg^{-1} K^{-1} and ρ_w=1000 kg m^{-3} are the specific gas constant and density of water and T is the temperature. In the test simulations for sodium chloride particles (Sect. 2.3) using the OS Köhler model, σ was calculated by a parameterization (Pruppacher and Klett, 1997). In all simulations using the κ-Köhler model, σ was set to 0.072 J m^{-2} (Petters and Kreidenweis, 2007).

2.3 Model validation

To validate the cloud parcel model after implementation of the κ-Köhler approach, we have compared it against simulations with the OS Köhler model and against the results of an alternative cloud parcel model using sodium chloride particles as a surrogate for atmospheric aerosols (Segal and Khain, 2006).

The influence of the different Köhler model approaches was evaluated in test simulations for two cloud base updraft velocities (w=1.5 m s^{-1} and 3.0 m s^{-1}) with a total aerosol particle number concentration of N_{CN}=3000 cm^{-3} and a log-normal size distribution as specified by Segal and Khain (2006) with a geometric mean diameter of 60 nm and a standard deviation of σ=1.35. Figure 1 shows that the maximum supersaturations (S_{max}) as well as the cloud droplet number concentrations (N_{CD}) determined with the κ-Köhler model were slightly lower than with the OS reference model. The differences can be attributed to simplifying assumptions in the κ-Köhler model that lead to deviations in the critical supersaturation for CCN activation (Rose et al., 2008a). Nevertheless, the small relative deviations in S_{max} and N_{CD} (<3%) confirm that the κ-Köhler approach is suitable for describing the hygroscopic properties and CCN activity of atmospheric aerosols in the cloud parcel model.

The validity of the cloud parcel model with the κ-Köhler approach was also confirmed by further model simulations with N_{CN}=800–3600 cm^{-3} and w=0.5–3.5 m s^{-1} with a κ of 1.28 representing NaCl. The resulting cloud droplet concentrations shown in Fig. 2 are in fair agreement with the results of Segal and Khain (2006, Fig. 6f) who investigated CCN activation with an alternative air parcel model with spectral description of

warm cloud microphysics. At low N_{CN}, the cloud droplet number concentrations were up to ~15% higher in our model, but at high N_{CN} they were essentially the same as in Segal and Khain (2006, Fig. 6f).

3 Results and discussion

3.1 Different regimes of CCN activation

To probe and characterize the influence of aerosol particle number concentration and updraft velocity on CCN activation and droplet formation at the base of pyro-convective clouds, we have performed cloud parcel model simulations assuming a mono-modal particle size distribution characteristic for young biomass burning aerosols. The dry particle size distribution is determined by an accumulation mode with a count median or geometric mean diameter of D_g=120 nm, a geometric standard deviation of σ_g=1.5 (Reid et al., 2005; Janhäll et al., 2009), and the hygroscopic properties are described by an effective hygroscopicity parameter of 0.2 (Andreae and Rosenfeld, 2008; Rose et al., 2008b; Pöschl et al., 2009). The effects of variations in hygroscopicity will be addressed below (Sect. 3.2). In a series of 961 model runs the updraft velocity and the initial number concentration of aerosol particles have been varied systematically over the range of w=0.5–20 m s^{-1} and N_{CN}=1–100×10^3 cm^{-3}.

Figure 3 shows the number concentration of cloud droplets, N_{CD}, that are formed at the cloud base as a function of w and N_{CN}. Note, that N_{CN} as used in this study effectively corresponds to $N_{CN,30}$, i.e. the number of aerosol particles larger than 30 nm. The corresponding activated fractions of aerosol particles and the maximum water vapor supersaturations reached in the ascending air masses (S_{max}) are shown in Figs. 4 and 5, respectively.

The N_{CD} isolines (isopleths) shown in Fig. 3 exhibit three distinctly different regimes of CCN activation and cloud droplet formation: (1) an aerosol-limited regime in the upper left sector of the plot; (2) an updraft-limited regime in the lower right sector; and

ACPD
9, 8635–8665, 2009

(3) an aerosol- and updraft-sensitive regime along the diagonal from the lower left to the upper right corner (ridge of N_{CD} isopleths). Note that the appearance of the cloud droplet isopleth plot is similar to that of the ozone isopleth plots which are widely used in atmospheric chemistry to distinguish and describe the so-called NO_x- and VOC-limited regimes of ozone production and concentration (Seinfeld and Pandis, 2006, p. 236).

The aerosol-limited regime of CCN activation is characterized by a relatively high ratio between the updraft velocity and particle number concentration ($w/N_{CN} > \approx 10^{-3}\,\mathrm{m\,s^{-1}/(cm^{-3})}$, Fig. 3), by a high activated fraction of aerosol particles ($N_{CD}/N_{CN} > \approx 90\%$, Fig. 4), and by high maximum values of water vapor supersaturation ($S_{max} > 0.5\%$, Fig. 5). In this regime, N_{CD} is directly proportional to N_{CN} ($\partial N_{CD}/\partial N_{CN} \approx 1$) and practically independent of w (isolines parallel to y-axis; $\partial N_{CD}/\partial w \approx 0$). The high updraft velocities lead to maximum supersaturations large enough to activate nearly all aerosol particles except very small ones at the lower end of the size-distribution (critical dry diameter of CCN activation $< \approx 60$ nm).

The updraft-limited regime is characterized by a relatively low ratio between the updraft velocity and particle number concentration ($w/N_{CN} < \approx 10^{-4}\,\mathrm{m\,s^{-1}/(cm^{-3})}$, Fig. 3), by a low activated fraction of aerosol particles ($N_{CD}/N_{CN} < \approx 20\%$, Fig. 4), and by low maximum values of water vapor supersaturation ($S_{max} < 0.2\%$, Fig. 5). In this regime N_{CD} exhibits a linear dependence on w ($\partial N_{CD}/\partial w \approx 2\times10^{3}\,\mathrm{cm^{-3}/m\,s^{-1}}$) and a very weak dependence on N_{CN} (small slope of isolines; $\partial N_{CD}/\partial N_{CN} \approx 0.02$). Due to the relatively low updraft velocities and high aerosol concentrations, the maximum supersaturations are so small that only large particles in the upper half of the size distribution are activated (critical dry diameter $> \approx 120$ nm).

The aerosol- and updraft-sensitive regime is characterized by intermediate values of the ratio between the updraft velocity and particle number concentration ($w/N_{CN} \approx 0.5\times10^{-3}\,\mathrm{m\,s^{-1}\,cm^{3}}$, Fig. 3), of the activated fraction of aerosol particles ($N_{CD}/N_{CN} \approx 20$–90%, Fig. 4), and of the maximum values of water vapor supersaturation ($S_{max} \approx 0.2$–0.5%, Fig. 5). In this regime N_{CD} exhibits non-linear dependences on both w and N_{CN} (strong curvature of isolines; $\partial N_{CD}/\partial w \approx (0\text{–}2)\times10^{3}\,\mathrm{m\,s^{-1}\,cm^{3}}$;

$\partial N_{CD}/\partial N_{CN} \approx 0.4$–1). Depending on the maximum supersaturations, the critical dry diameter for CCN activation ranges from well below up to the maximum of the aerosol particle size distribution (~60–120 nm).

The key features of the three regimes of CCN activation illustrated in Figs. 3–5 are not specific for young biomass burning aerosols and pyro-convective conditions but likely to apply also for other types of aerosols and meteorological conditions. This is due to the fairly similar CCN properties of aerosols in most regions of the world (Andreae and Rosenfeld, 2008; Rose et al., 2008a; Gunthe et al., 2009) and confirmed by sensitivity studies with different aerosol size distributions (not shown) and effective hygroscopicities (Sect. 3.2).

In the atmosphere, aerosol-limited conditions of CCN activation with high updraft velocities and low aerosol concentrations may occur in deep convection of clean air over tropical oceans and remote continental regions, as well as in thunderstorms in maritime air over land with strong vertical forcing of clean air masses (Murphey et al., 2005). Updraft-limited CCN activation with low updraft velocities and high aerosol concentrations is likely to occur in shallow convection of polluted air over locations or regions with strong sources of aerosols such as biomass burning and fossil fuel combustion in agricultural regions and mega-cities (Mönkkönen et al., 2005; Molina et al., 2007; Zhang et al., 2008; Rose et al., 2008; Wiedensohler et al., 2009). Aerosol- and updraft-sensitive conditions of CCN activation can occur in a wide range of regions and meteorological situations with low/moderate updraft velocities and aerosol concentrations (shallow convection in moderately polluted continental air), as well as in the very high updraft velocities and aerosol concentrations typical for pyro-convection.

For pyro-convective clouds with $w \approx 5$–$20\,\mathrm{m\,s^{-1}}$ and $N_{CN} \approx 10^4$–$10^5\,\mathrm{cm^{-3}}$, our model results indicate very high droplet number concentrations at the cloud base ($N_{CD} \approx (0.5$–$4) \times 10^4\,\mathrm{cm^{-3}}$; Fig. 3). The corresponding maximum water vapor supersaturations and activated fractions of aerosol particles are in the range of 0.2–0.5% and 20–80%, respectively (Figs. 4 and 5). The activated particle fractions are substantially higher than assumed in earlier model studies of pyro-convective clouds (5%, Trentmann et

ACPD
9, 8635–8665, 2009

al., 2006). On the other hand, the linear extrapolation of our results to extreme pyro-convective conditions (N_{CN}=4×10^5 cm^{-3}, w=20 m s^{-1}) is consistent with the results of Chuang et al. (1992: S_{max}=0.15, N_{CD}/N_{CN}=16%).

The cloud droplet number concentrations presented in this study are exceptionally high compared to non-pyro-convective clouds. These high concentrations of small cloud droplets at the cloud base have important effects on the subsequent microphysical evolution of pyro-convective clouds, because the cloud droplet collision efficiency is quite low for small droplets (Pinsky et al., 2001). Under these conditions, the production of larger cloud droplets by collision-coalescence and hence the formation of warm rain is suppressed. Therefore the liquid water in the cloud can be lofted into higher atmospheric regions, where, by release of latent heat through freezing processes, the strength of the convection can be enhanced (Rosenfeld et al., 2008). But, because of the fast updrafts in pyro-clouds combined with the small droplet size, ice formation is dominated by homogeneous freezing around −38°C, producing a large number of small ice particles. This results in the suppression of precipitation even from the ice phase mechanisms (Luderer et al., 2006; Rosenfeld et al., 2007). Note, that despite the enormous energy release by wildfires, the release of latent heat from condensation and freezing dominates the energy budget of pyro-clouds (Trentmann et al., 2006).

When an aerosol particle is activated to a cloud droplet it is also scavenged from the atmosphere (nucleation scavenging). The remaining fraction of the aerosol particles is transported as interstitial aerosol in the pyro-cloud and, unless they are scavenged by impaction with hydrometeors, they will be released into the atmosphere in the outflow region of the pyro-cloud, which can be as high as the upper troposphere or the lower stratosphere (e.g., Fromm et al., 2005). To quantify the number of aerosol particles in the outflow region of pyro-clouds, full three-dimensional simulations of pyro-clouds are required that take into account the interaction of aerosol particles and hydrometeors. Combining pyro-convective modeling activities (e.g., Trentmann et al., 2006; Luderer et al., 2007) with the investigation of aerosol-cloud interactions in convective clouds (e.g., Ekman et al., 2008) should help to better quantify the amount of aerosol deposited in

ACPD
9, 8635–8665, 2009

the UT/LS region by pyro-convection.

3.2 Aerosol particle hygroscopicity and size distribution

To probe and characterize the influence of aerosol particle hygroscopicity on CCN activation at the base of pyro-convective clouds, we have performed additional cloud parcel simulations for exemplary points in the three different regimes of CCN activation (aerosol-limited; updraft-limited; aerosol- and updraft-sensitive; Fig. 3).

In these simulations we used the same model setup and input parameters as detailed above (Sect. 3.1), but for each of the three investigated combinations of w and N_{CN} we varied the effective hygroscopicity parameter from 0.001 to 0.6, covering the full range of κ values that have been reported from CCN measurements of continental aerosols. The global average value of κ in continental air is ~0.3; sulfate- or nitrate-rich particles have higher values (~0.4–0.6); biomass burning particles are mostly in the range of the $\kappa \approx 0.1$–0.3; and largely insoluble particles such as soot, primary biological particles and mineral dust are characterized by $\kappa < 0.1$ (Petters and Kreidenweis, 2007; Andreae and Rosenfeld, 2008; Rose et al., 2008b; Gunthe et al., 2009; Kreidenweis et al., 2009; Pöschl et al., 2009).

Figure 6a shows the model results of N_{CD} and S_{max} for exemplary conditions in the aerosol-limited regime ($w = 15\,m\,s^{-1}$, $N_{CN} = 1 \times 10^4\,cm^{-3}$). Under these conditions and for aerosol particles of medium or high hygroscopicity ($\kappa \geq 0.2$), the cloud droplet number concentration is practically independent of κ (plateau level in Fig. 6a). The relative differential quotient $(\Delta N_{CD}/N_{CD})/(\Delta\kappa/\kappa)$ is ≤ 0.06, i.e., a ~50% difference in κ would change N_{CD} by less than 3% (Table 1). For aerosol particles with low hygroscopicity ($0.05 < \kappa < 0.2$), the dependence of N_{CD} on κ is still modest, with relative differential quotients $(\Delta N_{CD}/N_{CD})/(\Delta\kappa/\kappa)$ in the range of 0.06–0.2. Only for particles with very low hygroscopicity ($\kappa < 0.05$), N_{CD} depends strongly on κ. The relative differential quotients $(\Delta N_{CD}/N_{CD})/(\Delta\kappa/\kappa)$ are ≥ 0.2, i.e., a ~50% difference in κ would change N_{CD} by more than 10% (Table 1).

Figure 6b shows the model results for exemplary conditions in the aerosol- and

updraft- sensitive regime (w=10 m s^{-1}, N_{CN}=5×10^4 cm^{-3}). The dependence of N_{CD} on κ is qualitatively similar to the aerosol-limited regime (Fig. 6a), but the relative differential quotients $(\Delta N_{CD}/N_{CD})/(\Delta\kappa/\kappa)$ are larger, i.e., differences in κ result in larger differences in N_{CD} and (Table 1). Note that at κ>0.4 the maximum supersaturation dropped below 0.2%, indicating a changeover into the updraft limited regime. At κ>0.45 strong wiggles/outliers in the curve of N_{CD} vs. κ indicate that the model resolution becomes a limiting factor under these conditions (low S, high N).

Figure 6c shows the model results for exemplary conditions in the updraft-limited regime (w=5 m s^{-1}, N_{CN}=8×10^4 cm^{-3}). Again the dependence of N_{CD} on κ is qualitatively similar to the aerosol-limited regime (Fig. 6a), but the relative differential quotients $(\Delta N_{CD}/\mathrm{N}_{CD})/(\Delta\kappa/\kappa)$ are smaller for particles with low hygroscopicity (0.05<κ<0.2) and larger for particles with medium or high hygroscopicity ($\kappa\geq$0.2, Table 1). Note, however, that at $\kappa\approx$0.12 the maximum supersaturations drop already below 0.2% and strong wiggles/outliers in the curve of N_{CD} vs. κ indicate that the model resolution becomes a limiting factor.

Overall, the results summarized in Table 1 and Fig. 6 show that within the range of effective hygroscopicity parameters that is characteristic for continental atmospheric aerosols ($\kappa\approx$0.05–0.6), N_{CD} depends only weakly on the actual value of κ. Only for aerosols with very low average hygroscopicity (κ<0.05, all regimes) and in the updraft-limited regime also for aerosols with higher than average hygroscopicity (κ>0.3, S_{max}<0.2%) did the relative differential quotients $(\Delta N_{CD}/N_{CD})/(\Delta\kappa/\kappa)$ exceed values of ~0.2, indicating that a 50% difference in κ would change N_{CD} by more than 10%. At κ<0.03 and in the updraft-limited regime at κ>0.5 ($S_{\mathrm{max}}\leq$0.1%) the relative differential quotients $(\Delta N_{CD}/N_{CD})/(\Delta\kappa/\kappa)$ exceeded values of ~0.4, indicating that a 50% difference in κ would change N_{CD} by more than 20%. These findings are consistent with earlier studies investigating the influence of aerosol chemical composition on CCN activation in cloud parcel models (e.g., Lance et al., 2004; Rissman et al., 2004; Ervens et al., 2005).

To test the dependence of our results on the assumed dry aerosol particle size dis-

ACPD
9, 8635–8665, 2009

tribution, we have performed additional cloud parcel simulations with size distributions differing from the standard biomass burning particle size distribution used above. Increasing the geometric mean diameter of the accumulation mode (D_g) from 120 nm to 130 nm, had practically no effect on N_{CD} in the aerosol-limited regime of CCN activation. In the aerosol- and updraft sensitive regime, the relative deviations increased with decreasing S_{max} from $\Delta N_{CD}/N_{CD}$<3% at S_{max}>0.3% to $\Delta N_{CD}/N_{CD}\approx$10% at $S_{max}\approx$0.2%. Only at S_{max}<0.1% in the updraft-limited regime did $\Delta N_{CD}/N_{CD}$ exceed 30%.

In another set of model simulations we added a coarse particle mode with $D_{g,c}$=5μm and $\sigma_{g,c}$=1.3, and we assigned different fractions of N_{CN} to this mode ($f_{N,c}=10^{-5}$ to 10^{-3}; Reid et al., 2005; Liu et al., 2008; Janhäll et al., 2009). With $f_{N,c}=10^{-5}$ and in the aerosol-limited regime, the coarse particle mode had practically no influence on N_{CD} ($\Delta N_{CD}/N_{CD}\approx$0). In the aerosol- and updraft-sensitive regime $\Delta N_{CD}/N_{CD}$ increased with decreasing S_{max} up to ~10% for $f_{N,c}=10^{-4}$ and ~30% for $f_{N,c}=10^{-3}$, respectively. At S_{max}<0.1% in the updraft-limited regime $\Delta N_{CD}/N_{CD}$ exceeded ~20% for $f_{N,c}=10^{-4}$ and ~70% for $f_{N,c}=10^{-3}$, respectively.

Overall, the sensitivity studies show that realistic changes in the dry particle size distribution are not likely to induce relative changes >3% in N_{CD} provided that S_{max}>0.3%. The calculated relative changes in N_{CD} exceeded 20% only in the updraft limited regime where S_{max} falls below 0.2%. Since pyro-convective clouds are mostly outside the updraft-limited regime and because our model setup sensitive to small changes at very low supersaturations, we did not further investigate the influence of coarse mode particles on CCN activation in the updraft limited regime. Nevertheless, we suggest and intend to investigate this aspect further with model studies and observational data for polluted mega-city regions, which are often in the updraft limited regime. For this purpose, we also suggest and intend to apply models that enable assigning different hygroscopic properties to accumulation mode and coarse mode particles, as the latter are likely to be less hygroscopic. Moreover, potential kinetic limitations of water vapor

ACPD
9, 8635–8665, 2009

uptake at the interface and into the bulk of aerosol particles have not been considered in the present study but need to be further explored and clarified (Nenes et al., 2001; Laaksonen et al., 2005; McFiggans et al., 2006; Pöschl et al., 2007, 2009; Engelhart et al., 2008; Ruehl et al., 2008; Asa-Awuku et al., 2009; Mikhailov et al., 2009; and references therein).

4 Conclusions

Based on cloud parcel model simulations, we found that CCN activation and cloud droplet formation can be classified into three regimes depending on the ratio between updraft velocity and particle number concentration (w/N_{CN}): (1) an aerosol-limited regime (high w/N_{CN}), (2) an updraft-limited regime (low w/N_{CN}) and (3) an aerosol- and updraft-sensitive regime (intermediate w/N_{CN}).

Overall, the model results suggest that the variability of initial cloud droplet number concentration in (pyro-)convective clouds is mostly dominated by the variability of updraft velocity and aerosol particle number concentration in the accumulation mode. Coarse mode particles and the variability of particle composition and hygroscopicity appear to be play important roles only at very low supersaturation in the updraft-limited regime of CCN activation (in particular at $S \leq 0.1\%$).

These conclusions are consistent with field measurements demonstrating that CCN number concentrations in pristine as well as in highly polluted continental air can be efficiently predicted with a constant average hygroscopicity parameter of $\kappa \approx 0.3$, whereby the relative deviations between modeled and measured CCN concentrations exceeded 50% only at very low supersaturations ($\leq 0.1\%$; Rose et al., 2008b; Gunthe et al., 2009). Thus, we suggest that further experimental and theoretical studies of CCN activation and cloud droplet formation should be focused primarily on the updraft-limited regime, low water vapor supersaturations and potential kinetic limitations of CCN activation.

Acknowledgements. This work has been supported by an International Max Planck Research School fellowship and by the the European integrated project on aerosol cloud climate and

air quality interactions (No 036833-2, EUCAARI). We thank A. Seifert, M. Lawrence, S. Janhäll, S. Gunthe and D. Rosenfeld for helpful discussions.

The service charges for this open access publication have been covered by the Max Planck Society.

References

Altaratz, O., Koren, I., Reisin, T., Kostinski, A., Feingold, G., Levin, Z., and Yin, Y.: Aerosols' influence on the interplay between condensation, evaporation and rain in warm cumulus cloud, Atmos. Chem. Phys., 8, 15–24, 2008, http://www.atmos-chem-phys.net/8/15/2008/.

Andreae, M. O., Artaxo, P., Fischer, H., Freitas, S. R., Gregoire, J.-M., Hansel, A., Hoor, P., Kormann, R., Krejci, R., Lange, L., Lelieveld, J., Lindinger, W., Longo, K., Peters, W., de Reus, M., Scheeren, B., Silva Dias, M. A. F., Ström, J, van Velthofen, P. F. J., and Williams, J.: Transport of biomass burning smoke to the upper troposphere by deep convection in the equatorial region, Geophys. Res. Lett., 28, 951–954, 2001

Andreae, M. O., Rosenfeld, D., Artaxo, P., Costa, A. A., Frank, G. P., Longo, K. M., and Silva-Dias, M. A. F.: Smoking Rain Clouds over the Amazon, Science, 303, 1337–1342, 2004.

Andreae, M. O. and Rosenfeld, D.: Aerosol-cloud-precipitation interactions. Part 1: The nature and sources of cloud-active aerosols, Earth Sci. Rev., 89(1–2), 13–41, doi:10.1016/j.earscirev.2008.03.001, 2008.

Asa-Awuku, A., Engelhart, G. J., Lee, B. H., Pandis, S. N., and Nenes, A.: Relating CCN activity, volatility, and droplet growth kinetics of β-caryophyllene secondary organic aerosol, Atmos. Chem. Phys., 9, 795–812, 2009, http://www.atmos-chem-phys.net/9/795/2009/.

Chuang, C. C., Penner, J. E., and Edwards, L. L.: Nucleation Scavenging of Smoke Particles and Simulated Drop Size Distributions over Large Biomass Fires, J. Atmos. Sci, 49(14), 1264–1275, 1992.

Cubison, M. J., Ervens, B., Feingold, G., Docherty, K. S., Ulbrich, I. M., Shields, L., Prather, K., Hering, S., and Jimenez, J. L.: The influence of chemical composition and mixing state of Los Angeles urban aerosol on CCN number and cloud properties, Atmos. Chem. Phys., 8,

5649–5667, 2008,
http://www.atmos-chem-phys.net/8/5649/2008/.
Diehl, K., Simmel, M., and Wurzler, S.: Numerical sensitivity studies on the impact of aerosol properties and drop freezing modes on the glaciation, microphysics, and dynamics of clouds, J. Geophys. Res., 111, D07202, doi:10.1029/2005JD005884, 2006.
Diehl, K., Simmel, M., and Wurzler, S.: Effects of drop freezing on microphysics of an ascending cloud parcel under biomass burning conditions, Atmos. Environ., 41, 303–314, 2007.
Ekman, A. M. L., Krejci, R., Engstrom, A., Ström, J., de Reus, M., Williams, J., Andreae, M. O.: Do organics contribute to small particle formation in the Amazonian upper troposphere?, Geophys. Res. Lett., 35, L17810, doi:10.1029/2008GL034970, 2008.
Ervens, B., Feingold, G., and Kreidenweis, S. M.: The influence of water soluble organic carbon on cloud drop number concentration, J. Geophys. Res., 110, D18211, doi:10.1029/2004JD005634, 2005
Engelhart, G. J., Asa-Awuku, A., Nenes, A., and Pandis, S. N.: CCN activity and droplet growth kinetics of fresh and aged monoterpene secondary organic aerosol, Atmos. Chem. Phys., 8, 3937–3949, 2008,
http://www.atmos-chem-phys.net/8/3937/2008/.
Feingold, G.: Modeling of the first indirect effect: Analysis of measurement requirements, Geophys. Res. Lett., 30(19), 1997, doi:10.1029/2003GL017967, 2003.
Fromm, M., Alfred, J., Hoppel, K., Hornstein, J., Bevilacqua, R., Shettle, E., Servranckx, R., Li, Z., and Stocks., B.: Observations of boreal forest fire smoke in the stratosphere by POAM III, SAGE II, and lidar in 1998, Geophys. Res. Lett., 27(9), 1407–1410, 2000.
Fromm, M. and Servranckx, R.: Transport of forest fire smoke above the tropopause by supercell convection, Geophys. Res. Lett., 30(10), 1542, doi:10.1029/2002GL016820, 2003.
Fromm, M., Bevilacqua, R., Servranckx, R., Rosen, J., Thayer, J. P., Herman, J., and Larko, D., Pyro-cumulonimbus injection of smoke to the stratosphere: Observations and impact of a super blowup in northwestern Canada on 3-4 August 1998, J. Geophys. Res., 110, D08205, doi:10.1029/2004JD005350, 2005.
Gunthe, S. S., King, S. M., Rose, D., Chen, Q., Roldin, P., Farmer, D. K., Jimenez, J. L., Artaxo, P., Andreae, M. O., Martin, S. T., and Pöschl, U.: Cloud condensation nuclei in pristine tropical rainforest air of Amazonia: size-resolved measurements and modeling of atmospheric aerosol composition and CCN activity, Atmos. Chem. Phys. Discuss., 9, 3811–3870, 2009,

http://www.atmos-chem-phys-discuss.net/9/3811/2009/.
Hegg, D. A.: Dependence of Marine Stratocumulus Formation on Aerosols, Geophys. Res. Lett., 26(10), 1429–1432, 1999.
Helsper, C., Fissan, H. J., Muggli, J., and Scheidweiler, A.: Particle number distribution of aerosols from test fires, J. Atmos. Sci., 11, 439–446, 1980.
Hjelmfelt, M. R., Farley, R. D., and Chen, P. C. S.: A preliminary numerical study into the effects of coal development on cloud and precipitation processes in the Northern Great Plains, J. Appl. Meteorol., 17(6), 846–857, 1978.
IAPSAG: International aerosol precipitation science assessment group (IAPSAG): Aerosol pollution impact on precipitation: a scientific review, 2007.
IPCC: Climate Change 2007: The Physical Science Basis. Contribution of Working Group I to the Fourth Assessment Report of the Intergovernmental Panel on Climate Change, edited by: Solomon, S., Qin, D., Manning, M., Chen, Z., Marquis, M., Averyt, K., Tignor, M., and Miller, H. L., 996 pp., Cambridge University Press, Cambridge and New York, 2007.
Janhäll, S., Andreae, M. O., and Pöschl, U.: Biomass burning aerosol emissions from wildfires: particle number and mass emission factors and size distributions, Atmos. Chem. Phys., submitted, 2009.
Jiang, H. J., Wang, B., Goya, K., Hocke, K., Eckermann, S. D., Ma, J., Wu, D. L., and Read W. G.: Geographical distribution and interseasonal variability of tropical deep convection: UARS MLS observations and analyses, J. Geophys. Res., 109, D03111, doi:10.1029/2003JD003756, 2004.
Kivekas, N., Kerminen, V. M., Anttila, T., Korhonen, H., Lihavainen, H., Komppula, M., and Kulmala, M.: Parameterization of cloud droplet activation using a simplified treatment of the aerosol number size distribution, J. Geophys. Res., 113(D15), D15207, doi:10.1029/2007JD009485, 2008.
Khain, A. P., BenMoshe, N., and Pokrovsky, A.: Factors determining the impact of aerosols on surface precipitation from clouds: An attempt at classification, J. Atmos. Sci., 65, 1721–1748, 2008.
Kreidenweis, S. M., Petters, M. D., and Chuang, P. Y.: Cloud particle precursors, in: Clouds in the perturbed climate system – their relationship to energy balance, atmospheric dynamics, and precipitation, edited by: Heintzenberg, J. and Charlson, R. J., MIT Press, Cambridge, UK, 291–317, 2009.
Laaksonen, A., Vesala, T., Kulmala, M., Winkler, P. M., and Wagner, P. E.: Commentary on

cloud modelling and the mass accommodation coefficient of water, Atmos. Chem. Phys., 5, 461–464, 2005, http://www.atmos-chem-phys.net/5/461/2005/.

Lance, S., Nenes, A., and Rissman, T. A.: Chemical and dynamical effects on cloud droplet number: Implications for estimates of the aerosol indirect effect, J. Geophys. Res., 109(D22), D22208, doi:10.1029/2004JD004596, 2004.

Liu, S.,Hu, M., Wu, Z., Wehner, B.Wiedensohler, A., and Cheng, Y.: Aerosol number size distribution and new particle formation at a rural/coastal site in Pearl River Delta (PRD) of China, Atmos. Environ., 42, 6275–6283, 2008.

Lohmann, U., Broekhuizen, K., Leatich, R. Shantz, N., and Abbatt, J.: How efficient is cloud droplet formation of organic aerosols, Geophys. Res. Lett., 31, L05108, doi:10.1029/2003GL018999, 2004.

Luderer, G., Trentmann, J., Winterrath, T., Textor, C., Herzog, M., Graf, H. F., and Andreae, M. O.: Modeling of biomass smoke injection into the lower stratosphere by a large forest fire (Part II): sensitivity studies, Atmos. Chem. Phys., 6, 5261–5277, 2006, http://www.atmos-chem-phys.net/6/5261/2006/.

McFiggans, G., Artaxo, P., Baltensperger, U., Coe, H., Facchini, M. C., Feingold, G., Fuzzi, S., Gysel, M., Laaksonen, A., Lohmann, U., Mentel, T. F., Murphy, D. M., O'Dowd, C. D., Snider, J. R., and Weingartner, E.: The effect of physical and chemical aerosol properties on warm cloud droplet activation, Atmos. Chem. Phys., 6, 2593–2649, 2006, http://www.atmos-chem-phys.net/6/2593/2006/.

Mikhailov, E., Vlasenko, S., Martin, S. T., Koop, T., and Pöschl, U.: Amorphous and crystalline aerosol particles interacting with water vapor – Part 1: Microstructure, phase transitions, hygroscopic growth and kinetic limitations, Atmos. Chem. Phys. Discuss., 9, 7333–7412, 2009, http://www.atmos-chem-phys-discuss.net/9/7333/2009/.

Molina, L. T., Kolb, C. E., de Foy, B., Lamb, B. K., Brune, W. H., Jimenez, J. L., Ramos-Villegas, R., Sarmiento, J., Paramo-Figueroa, V. H., Cardenas, B., Gutierrez-Avedoy, V., and Molina, M. J.: Air quality in North America's most populous city – overview of the MCMA-2003 campaign, Atmos. Chem. Phys., 7, 2447–2473, 2007, http://www.atmos-chem-phys.net/7/2447/2007/.

Mönkkönen, P., Koponen, I. K., Lehtinen, K. E. J., Hämeri, K., Uma, R., and Kulmala, M.: Measurements in a highly polluted Asian mega city: observations of aerosol number size

distribution, modal parameters and nucleation events, Atmos. Chem. Phys., 5, 57–66, 2005, http://www.atmos-chem-phys.net/5/57/2005/.
Murphey, H. V., Wakimoto, R. M., Flamant, C., and Kingsmill., D. E.: Dryline on 19 June 2002 during IHOP. Part I: Airborne Doppler and LEANDRE II Analyses of the Thin Line Structure and Convection Initiation, Mon. Weather Rev., 134, 406–430, 2006.
Nenes, A., Ghan, S., Abdul-Razzak, H., Chuang, P. Y., and Seinfeld, J. H.: Kinetic limitations on cloud droplet formation and impact on cloud albedo, Tellus, 53(2), 133–149, 2001.
Penner, J. E., Dong, X., and Chen, Y.: Observational evidence of a change in radiative forcing due to the indirect aerosol effect, Nature, 427, 231–234, 2004.
Petters, M. D. and Kreidenweis, S. M.: A single parameter representation of hygroscopic growth and cloud condensation nucleus activity, Atmos. Chem. Phys., 7, 1961–1971, 2007, http://www.atmos-chem-phys.net/7/1961/2007/.
Phillips, V. T. J., Donner, L. J., and Garner, S. T.: Nucleation processes in deep convection simulated by a cloud-system-resolving model with double-moment bulk microphysics, J. Atmos. Sci., 64, 738–761, 2007.
Pinsky M., Khain A., and Shapiro, M.: Collision efficiency of drops in a wide range of Reynolds numbers: Effects of pressure on spectrum evolution, J. Atmos. Sci., 58, 742–764, 2001.
Pitzer, K. S. and Mayorga, G.: Thermodynamics of electrolytes. II. Acitivity and osmotic coefficients for strong electrolytes with one or both ions univalent, J. Phys. Chem., 77, 2300–2308, 1973.
Pöschl, U., Rudich, Y., and Ammann, M.: Kinetic model framework for aerosol and cloud surface chemistry and gas-particle interactions – Part 1: General equations, parameters, and terminology, Atmos. Chem. Phys., 7, 5989–6023, 2007, http://www.atmos-chem-phys.net/7/5989/2007/.
Pöschl, U., Rose, D., and Andreae M. O.: Climatologies of cloud-related aerosols – Part 2: Particle hygroscopicity and cloud condensation nucleus activity, in: Clouds in the perturbed climate system – Their relationship to energy balance, atmospheric dynamics, and precipitation, edited by: Heintzenberg, J. and Charlson, R. J., MIT Press, Cambridge, UK, 58–72, 2009.
Posselt, R. and Lohmann, U.: Influence of Giant CCN on warm rain processes in the ECHAM5 GCM, Atmos. Chem. Phys., 8, 3769–3788, 2008, http://www.atmos-chem-phys.net/8/3769/2008/.
Pruppacher, H. R. and Klett, J. D.: Microphysics of clouds and precipitation, Kluwer Academics

Publishers, UK, 1997.
Reid, J. S. and Hobbs, P. V.: Physical and optical properties of young smoke from individual biomass fires in Brazil, J. Geophys. Res., 103, 32013–32030, 1998.
Reid, J. S., Koppmann, R., Eck, T. F., and Eleuterio, D. P.: A review of biomass burning emissions part II: intensive physical properties of biomass burning particles, Atmos. Chem. Phys., 5, 799–825, 2005, http://www.atmos-chem-phys.net/5/799/2005/.
Rissmann, T. A., Nenes, A. and Seinfeld, J. H.: Chemical amplification (or dampening) if the Towmey effect: Conditions derived from droplet activation theory, J. Atmos. Sci., 61(8), 919–930, 2004.
Rose, D., Gunthe, S. S., Mikhailov, E., Frank, G. P., Dusek, U., Andreae, M. O., and Pöschl, U.: Calibration and measurement uncertainties of a continuous-flow cloud condensation nuclei counter (DMT-CCNC): CCN activation of ammonium sulfate and sodium chloride aerosol particles in theory and experiment, Atmos. Chem. Phys., 8, 1153–1179, 2008a, http://www.atmos-chem-phys.net/8/1153/2008/.
Rose, D., Nowak, A., Achtert, P., Wiedensohler, A., Hu, M., Shao, M., Zhang, Y., Andreae, M. O., and Pöschl, U.: Cloud condensation nuclei in polluted air and biomass burning smoke near the mega-city Guangzhou, China – Part 1: Size-resolved measurements and implications for the modeling of aerosol particle hygroscopicity and CCN activity, Atmos. Chem. Phys. Discuss., 8, 17343–17392, 2008b, http://www.atmos-chem-phys-discuss.net/8/17343/2008/.
Rosenfeld, D.: Suppression of rain and snow by urban and industrial air pollution, Science, 287, 5459, 1793–1796, 2000.
Rosenfeld, D.: Aerosols, clouds, and climate, Science, 312, 1323–1324, 2006.
Rosenfeld, D., Fromm, M., Trentmann, J., Luderer, G., Andreae, M. O., and Servranckx, R.: The Chisholm firestorm: observed microstructure, precipitation and lightning activity of a pyro-cumulonimbus, Atmos. Chem. Phys., 7, 645–659, 2007, http://www.atmos-chem-phys.net/7/645/2007/.
Rosenfeld, D., Lohmann, U., Raga, G. B., O'Dowd, C. D., Kulmala, M., Fuzzi, S., Reissell, A., and Andreae, M. O., Flood or drought: How do aerosols affect precipitation?, Science, 321, 1309–1313, 2008.
Ruehl, C. R., Chuang, P. Y., and Nenes, A.: How quickly do cloud droplets form on atmospheric particles?, Atmos. Chem. Phys., 8, 1043–1055, 2008,

http://www.atmos-chem-phys.net/8/1043/2008/.
Segal, Y. and Khain, A.: Dependence of droplet concentration on aerosol conditions in different cloud types: Application to droplet concentration parameterization of aerosol conditions, J. Geophys. Rev., 111, D15204, doi:10.1029/2005JD006561, 2006.
Seinfeld, J. H. and Pandis, S. N.: Atmospheric chemistry and physics, Wiley & Sons, 2006.
Simmel, M. and Wurzler, S.: Condensation and activation in sectional cloud microphysical models, Atmos. Res., 80, 218–236, 2005.
Simmel, M., Trautmann, T., and Tetzlaff, G.: Numerical solution of the stochastic collection equation – comparison of the Linear Discrete Method with other methods, Atmos. Res., 61, 135–148, 2002.
Trentmann, J., Luderer, G., Winterrath, T., Fromm, M. D., Servranckx, R., Textor, C., Herzog, M., Graf, H.-F., and Andreae, M. O.: Modeling of biomass smoke injection into the lower stratosphere by a large forest fire (Part I): reference simulation, Atmos. Chem. Phys., 6, 5247–5260, 2006, http://www.atmos-chem-phys.net/6/5247/2006/.
Wang, P. K.: Moisture plumes above thunderstorm anvils and their contributions to cross-tropopause transport of water vapour in midlatitudes, J. Geophys. Res., 108(D6), 4194, doi:10.1029/2002JD002581, 2003.
Wiedensohler, A., Cheng, Y. F., Nowak, A., Wehner, B., Achtert, P., Berghof, M., Birmili, W., Wu, Z. J., Hu, M., Zhu, T., Takegawa, N., Kita, K., Kondo, Y., Lou, S. R., Hofzumahaus, A., Holland, F., Wahner, A., Gunthe, S. S., Rose, D., and Pöschl, U.: Rapid Aerosol Particle Growth and Increase of Cloud Condensation Nucleus (CCN) Activity by Secondary Aerosol Formation: a Case Study for Regional Air Pollution in North Eastern China, J. Geophys. Res., accepted, 2009.
Zhang, Y. H., Hu, M., Zhong, L. J., Wiedensohler, A., Liu, S. C., Andreae, M. O., Wang, W., and Fan, S. J.: Regional integrated experiments on air quality over Pearl River Delta 2004 (PRIDE-PRD2004): Overview., Atmos. Environ., 42(25), 6157–6173, 2008.

Table 1. Relative differential quotients $(\Delta N_{CD}/N_{CD})/(\Delta\kappa/\kappa)$ characterizing the dependence of cloud droplet number concentration (N_{CD}) on aerosol particle hygroscopicity (κ) in the aerosol-limited, aerosol- and updraft-sensitive, and updraft-limited regimes of CCN activation. Numerical values correspond to the exemplary scenarios illustrated in Fig. 6.

κ	Aerosol-limited regime (S_{max}>0.5%)		Aerosol- and updraft-sensitive regime (S_{max}=0.2–0.5%)		Updraft-limited regime (S_{max}<0.2%)	
	N_{CD},10^3 cm^{-3}	$(\Delta N_{CD}/N_{CD})/(\Delta\kappa/\kappa)$	N_{CD},10^3 cm^{-3}	$(\Delta N_{CD}/N_{CD})/(\Delta\kappa/\kappa)$	N_{CD},10^3 cm^{-3}	$(\Delta N_{CD}/N_{CD})/(\Delta\kappa/\kappa)$
0.025	6.0	0.50	14.0	0.50	8.0	0.50
0.05	7.5	0.23	16.5	0.22	9.6	0.10
0.1	8.4	0.12	19.0	0.21	10.2	0.06
0.2	8.9	0.06	21.0	0.10	10.5	0.10
0.3	9.1	0.03	22.0	0.08	11.0	0.22
0.4	9.2	0.02	23.0	0.11	13.0	0.30
0.5	9.3	0.02	24.0	0.14	13.3	0.41

ACPD
9, 8635–8665, 2009

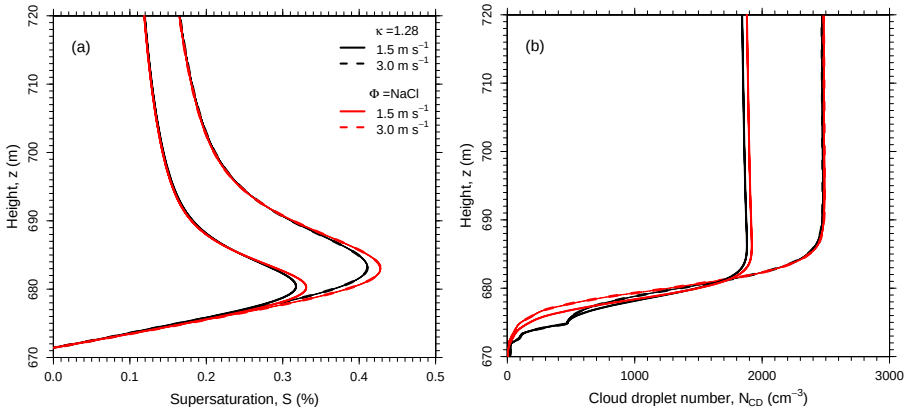

Fig. 1. Exemplary vertical profiles of **(a)** water vapor supersaturation (S, %) and **(b)** cloud droplet number concentration (N_{CD}, cm^{-3}) simulated with different Köhler model approaches: osmotic coefficient model (red lines) and κ-Köhler model (black lines). The updraft velocity was set to w=1.5 m s^{-1} (solid lines) or w=3.0 m s^{-1} (dashed lines), and the initial aerosol particle number concentration was set to N_{CN}=3000 cm^{-3} with particle properties as specified by Segal and Khain (2006).

ACPD
9, 8635–8665, 2009

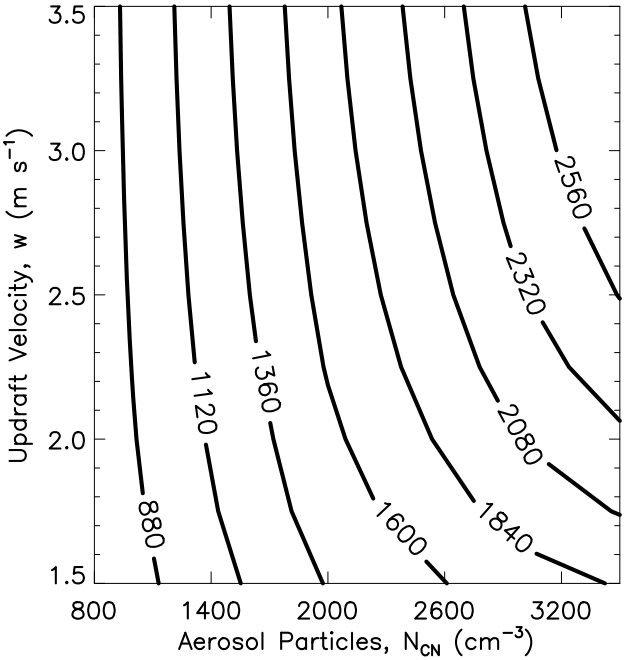

Fig. 2. Cloud droplet number concentrations (N_{CD}, cm^{-3}; isolines) calculated as a function of updraft velocity (w, m s^{-1}) and initial aerosol particle number concentration (N_{CN}, cm^{-3}) with particle properties as specified by Segal and Khain (2006).

ACPD
9, 8635–8665, 2009

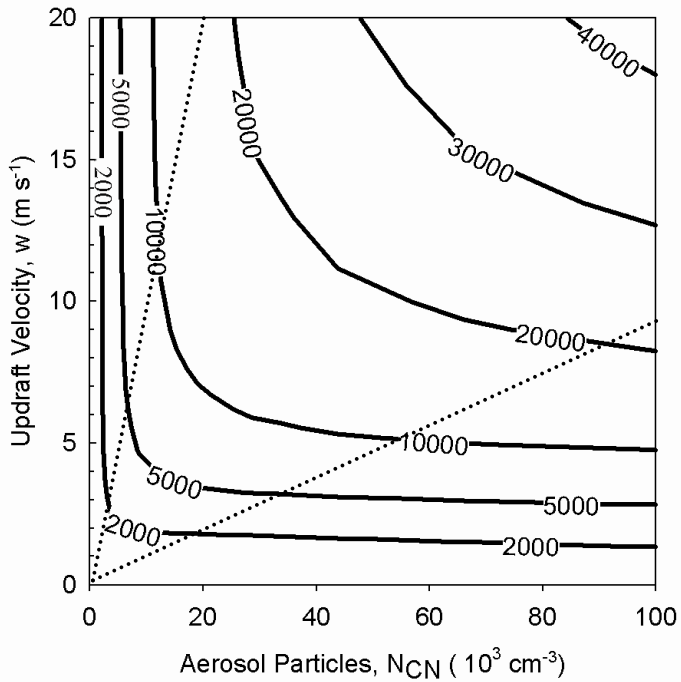

Fig. 3. Cloud droplet number concentrations (N_{CD}, cm^{-3}; isolines) calculated as a function of updraft velocity (w, $m\,s^{-1}$) and initial aerosol particle number concentration (N_{CN}, cm^{-3}). Dotted lines indicate borders between different regimes.

ACPD
9, 8635–8665, 2009

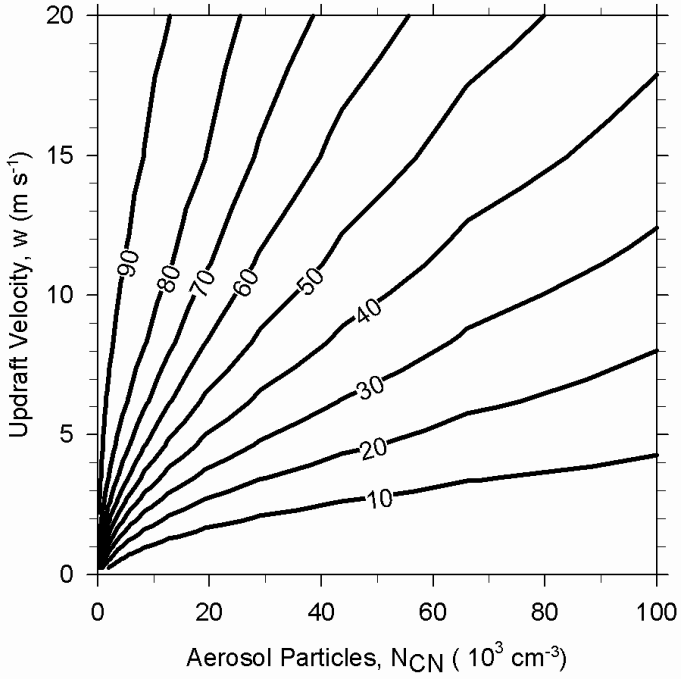

Fig. 4. Fraction of activated aerosol particles (N_{CD}/N_{CN}, %, isolines) calculated as a function of updraft velocity (w, m s^{-1}) and initial aerosol particle number concentration (N_{CN}, cm^{-3}).

ACPD
9, 8635–8665, 2009

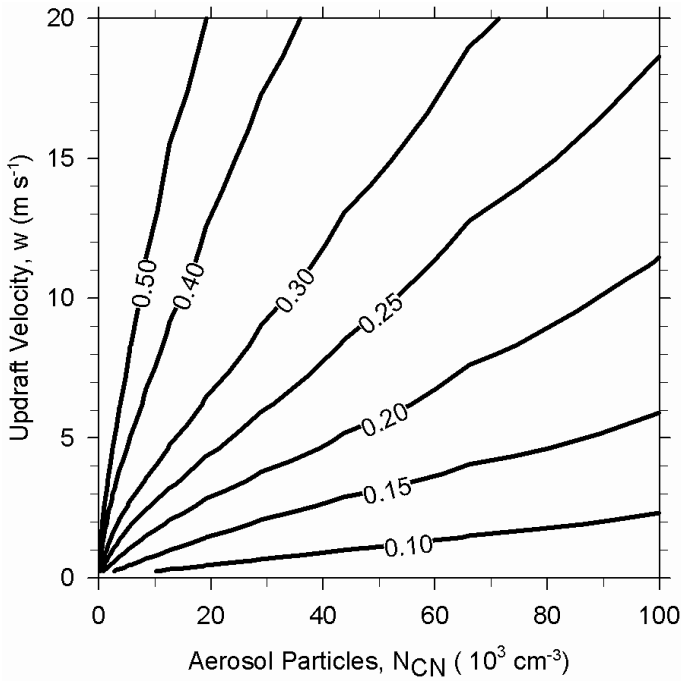

Fig. 5. Maximum supersaturation (S_{max}, %, isolines) calculated as a function of updraft velocity (w, m s^{-1}) and initial aerosol particle number concentration (N_{CN}, cm^{-3}).

ACPD
9, 8635–8665, 2009

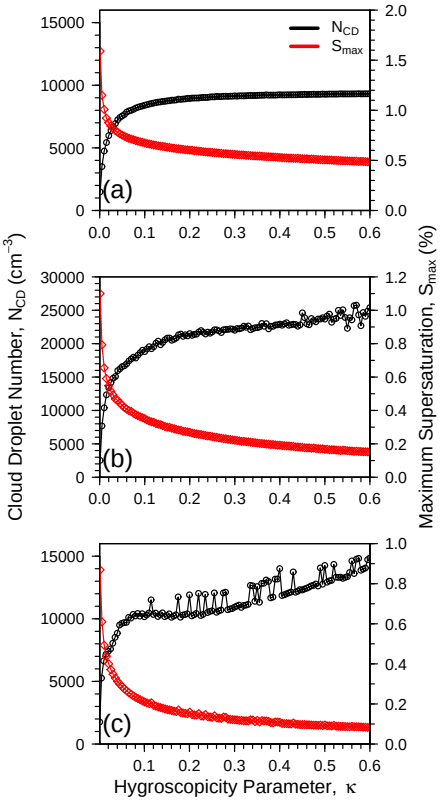

Fig. 6. Dependence of cloud droplet number concentrations (N_{CD}, cm^{-3}, black) and maximum supersaturations (S_{max}, %, red) on aerosol particle hygroscopicity (κ=0.005–0.6): **(a)** aerosol-limited regime (w=15 m s^{-1} and N_{CN}=1×10^4 cm^{-3}); **(b)** aerosol- and updraft-sensitive regime (w=10 m s^{-1} and N_{CN}=5×10^4 cm^{-3}); **(c)** updraft-limited regime (w=5 m s^{-1} and N_{CN}=8×10^4 cm^{-3}).

ACPD
9, 8635–8665, 2009